A CONSISTENT NUCLEAR MODEL FOR COMPOUND AND PRECOMPOUND REACTIONS WITH CONSERVATION OF ANGULAR MOMENTUM

C. Y. Fu
Oak Ridge National Laboratory
Oak Ridge, Tennessee 37830, USA

The exciton model is modified such that it automatically reduces to the usual evaporation formula after equilibrium has been reached. The result is further modified to conserve angular momentum in a form compatible with the Hauser-Feshbach formula. This allows a consistent description of intermediate excitations from which tertiary reaction cross sections can be calculated for transitions to discrete residual levels with known spins and parities. Level densities used for the compound component of reaction cross sections are derived from direct summation of the particle-hole state densities used for the precompound component.

[Nuclear reactions ^{27}Al, ^{46,48}Ti, ^{51}V, ^{50,52}Cr, ^{54,56}Fe, ^{58,60}Ni, ^{63,65}Cu, ^{93}Nb, E = 14.6 MeV. Calculated $\sigma(n,xn)$, (n,xp), $(n,x\alpha)$, $\sigma(E_n)$, (E_p), (E_α). Hauser-Feshbach and precompound analysis.]

Introduction

Development of fusion energy calls for substantial improvement in the knowledge of neutron cross sections in the energy range from a few MeV to about 40 MeV.[1] In this energy range, the multi-step Hauser-Feshbach model with precompound effects is the most versatile and is considered an indispensible theoretical tool for cross-section evaluations.[2] In analyzing cross sections such as hydrogen and helium productions from 14-MeV neutron-induced reactions, we showed[3] that spin and parity effects are more important in the second step of the calculation than in the first step. However, it is not straightforward to conserve angular momentum even in the first step because the presently available models for precompound reactions do not conserve or even recognize angular momentum. In addition the compound and precompound components are generally calculated in the first step from two physically different models, thus lacking a common basis for carrying out the calculation to the second step.

In this paper we develop a model capable of calculating the compound and precompound cross sections consistently and conserving angular momentum in both compound and precompound reactions. The model becomes that of Hauser-Feshbach[4] at low energies where the precompound effects are negligible. Level densities used for calculating the compound component are made consistent with those used for the precompound component.

Theory

A full derivation of the formula given below has been written up for publication elsewhere.[5] Here we only have enough space for a summary. We shall first write down the final formula and then explain the physical implications of the various components leading to its derivation.

The final formula is

$$\sigma_b(E,\varepsilon)d\varepsilon = \pi\lambda^2 \sum_{J\pi} g_J \sum_{s\ell} T^J_{s\ell} \frac{d\varepsilon}{D_{J\pi}} \sum_{s'\ell'} T^J_{s'\ell'} \Omega_b(I,E,U), \quad (1a)$$

where

$$D_{J\pi} = \sum_b \sum_{I\pi} \int_\varepsilon \sum_p \sum_{s'\ell'} T^J_{s'\ell'} \Omega_b(I,E,U) \quad (1b)$$

$$\Omega_b(I,E,U) = \sum_p D_b(p,E)\, \omega_b(p\text{-}1,h,I,U') + C(E)\, \rho_b(I,U') \quad (1c)$$

$$D_b(p,E) = \int_0^T P_b(p,h,t)dt/\omega(p,h,E) \quad (1d)$$

$$C(E) = \int_T^\infty P(p,h,t)dt/\omega(p,h,E) \quad (1e)$$

$$\rho_b(I,U') = \sum_p \omega_b(p\text{-}1,h,I,U') \quad , \quad (1f)$$

and the various components and notations are explained below.

The compound and precompound components are consistent if the precompound model automatically reduces to the compound model after equilibrium has been reached. This is achieved by introducing a set of master equations containing time-dependent particle-type distributions. Defining $P_b(p,h,t)$, the occupation probability, as the probability that the system will be found in a state with p particles and h holes of type b at time t, the master equations which describe the approach of the nucleus to statistical equilibrium are given by

$$\frac{d\,P_b(p,h,t)}{dt} = \left[\frac{P_b(p\text{-}1,h\text{-}1,t)}{P(p\text{-}1,h\text{-}1,t)}\frac{p\text{-}1}{p} + \frac{f_b(p)}{p}\right] P(p\text{-}1,h\text{-}1,t)\,\lambda_+(p\text{-}1,h\text{-}1,E)$$

$$+ \left[\frac{P_b(p+1,h+1,t)}{P(p+1,h+1,t)}\right] P(p+1,h+1,t)\,\lambda_-(p+1,h+1,E)$$

$$- P_b(p,h,t)\left[\lambda_+(p,h,E) + \lambda_-(p,h,E) + \int_0^{\varepsilon_{max}} X_b(p,h,\varepsilon)d\varepsilon\right] \quad (2a)$$

with

$$P(p,h,t) = \sum_b P_b(p,h,t) \quad (2b)$$

and

$$\sum_b f_b(p) = 1 \quad . \quad (2c)$$

The transition rates λ_+ and λ_- are given by Ribansky *et al.*[5] which contain an empirical residual two-body matrix element determined by Kalbach.[6] E is the total energy of the reacting system.

In the first term in Eq. (1l), $P(p\text{-}1,h\text{-}1,t)\,\lambda_+(p\text{-}1,h\text{-}1,E)$ represents the total transition rates from (p-1,h-1) states to (p,h) states. Among the p particles in the (p,h) states, (p-1) of them retain the old particle-type distribution $P_b(p\text{-}1,h\text{-}1,t)/P(p\text{-}1,h\text{-}1,t)$, and the newly created particle may have a different particle-type distribution given by $f_b(p)$, which will be determined analytically. Thus the compositions of particle types in the new (p,h) states are given by the quantity in the brackets.

DISCLAIMER

In the second term, $P(p+1,h+1,t)\ \lambda_b(p+1,h+1,E)$ represents the total transition rates from $(p+1,h+1)$ states to (p,h) states. The quantity in the brackets is the fraction of particle type b in the (p,h) states. If we assume that various types of particles annihilate with their respective holes at the same rate, then the compositions of various particles in the newly formed (p,h) states are the same as in the initial $(p+1,h+1)$ states.

The emission rates X_b are given by

$$X_b(p,h,\varepsilon)d\varepsilon = \frac{2S_b+1}{\pi^2\hbar^3}\mu_b\,\varepsilon\,\sigma_b(\varepsilon)d\varepsilon\,\frac{\omega_b(p-1,h,U)}{\omega(p,h,E)} \quad . \tag{3}$$

where S_b, μ_b, and ε are the spin, reduced mass, and kinetic energy of the emitted particle of type b; U is the residual nucleus excitation energy. Equation (3) differs from that of Kalbach[7] in the absence of the particle-type weighting factor $R_b(p)$. This weighting factor is now time dependent and is built into Eq. (2). The state densities $\omega(p,h,E)$ are given by Williams.[8]

The numerical values of $f_b(p)$ are determined by requiring that after equilibrium has been reached the system will stay in equilibrium. Our definition of equilibrium is

$$P_b(p,h,t \geq T)/\omega(p,h,E) = C(t,E) \tag{4}$$

where the equilibration time T is the time when all allowed states in the composite system are equally populated. This definition of equilibrium leads to

$$f_b(p) = \frac{1}{N} \tag{5}$$

where N is the number of particle types included in the calculation.

The initial conditions for numerical integration of Eq. (2) are given by

$$P_b(p,h,0) = \delta_{pp_o}\delta_{hh_o}\,q_b \quad , \tag{6}$$

where q_b is the fraction of particle type b in the states (p_o,h_o) at time 0. This fraction is previously contained in $R_b(p_o)$.

To conserve angular momentum it is necessary to write the occupation probability as $P_b(p,h,J,t)$ where J is the total spin of the reacting system. Eq. (1) was derived with this definition for the occupation probability. We shall not attempt to solve for this occupation probability. Instead we make the simplifying assumption that

$$\frac{P_b(p,h,J,t)}{\omega(p,h,J,E)} = \frac{P_b(p,h,t)}{\omega(p,h,E)} \tag{7}$$

so that Eq. (2) can be used directly. This has little to do with our goal of conserving angular momentum. What we have neglected are the angular momentum couplings among the p particles and h holes and their possible influence on the spreading widths and escaping widths. Solution of this problem is beyond our present purpose.

The spin dependent p-h state densities for the residual nuclei are given by

$$\omega(p,h,J,E) = \omega(p,h,E)\,\omega_n(J) \quad , \tag{8a}$$

where

$$\omega_n(J) = \frac{1}{2\sqrt{2\pi}\,\sigma_n^3}(2J+1)\,e^{-(J+\frac{1}{2})^2/2\sigma_n^2} \quad , \tag{8b}$$

with

$$\sigma_n^2 = 1.17\,nc/a \quad , \tag{8c}$$

where $a = \pi^2 g/6$, and c is a constant related to the moment of inertia.[9] Equation (8c) is derived by equating σ_n^2 to $c\tau$ where $\bar{n}$ is the most probable exciton number and τ is the nuclear temperature.[9]

The effective excitation energy U' is given by

$$U' = U - U_{p,h}$$

with

$$U_{p,h} = (h-1.5)\Delta + U_o$$

and[10]

$$\Delta = 12/\sqrt{A}$$

where U_o is the odd-even shift of Gilbert and Cameron[9] and A is the mass number. The pairing correction, $U_{p,h}$, reduces the p-h state densities given ty Williams[9] by a factor of 10 and makes their summation (over p or h) comparable to empirical descriptions such as those given by Gilbert and Cameron.[9]

Finally, converting all inverse reaction cross sections in the cross section formula given by Kalbach[6] into transmission coefficients, $T^U_{s\ell}$ and $T^U_{s'\ell'}$, where s, ℓ, s', ℓ' are the channel spins and orbital angular momenta of the incident and outgoing particles, we obtain Eq. (1). If instantaneous equilibration is assumed, Eq. (1) reduces to the usual Hauser-Feshbach formula. We emphasize that as long as comparable level densities are used, the compound part of our model, as obtained directly from the precompound model developed here, would yield identical results as the conventional compound model.

Parameter Determinations and Calculations

Calculations of neutron, proton, and alpha-particle production spectra for 14.6-MeV neutrons incident on thirteen isotopes are compared with experimental data.[11,12] Parameters of general validity are fixed beforehand. Two parameters are determined from calculations for ^{56}Fe and then used for predicting the other twelve isotopes.

Optical model parameters are taken from Wilmore and Hodgson[13] for neutrons, Becchetti and Greenlees[14] for protons, and Huizenga and Igo[15] for alpha-particles. Calculation of gamma-ray transmission coefficients was described previously in detail.[16] Level density parameters, a, c, and U_o, are calculated from the empirical formalism of Gilbert and Cameron[9] and used in Eq. (1f) as well as Eqs. (8a) to (8c). The single particle density g for each nucleus is calculated from the corresponding parameter a and thus has the effect of shell corrections, as given by Gilbert and Cameron.[9]

A few discrete levels are used for each residual nucleus in the binary step. These levels are given a weight $\Omega_b(I,E,U_c)/\rho(I,U')$, defined in Eqs. (1c) and (1f) with U_c being the continuum cutoff, such that continuity in the calculated spectra across U_c is maintained. A larger number of discrete levels in each residual nucleus is used in the second step such that more than 80% of decays by proton emission excite the discrete levels. Often only a few discrete levels are excited by the second outgoing particles in (n,np) and (n,nα) reactions. In such cases, the calculated tertiary-reaction cross sections are sensitive to the spacings and spins of the residual discrete levels.

The remaining parameters are k, the scale factor

for the residual two-body matrix elements,[7] and q_b, the fraction of particle type b in the states $(p_o;h_o)$ at time 0. A neutron incident on a nucleus sees N neutrons, Z protons, and a maximum of Z/2 alpha clusters. Introducing a parameter f as the clustering probability[7] for alpha particles and using $p_o = 2$ and $h_o = 1$, we have

$$b_n = 0.5\ N/A' + 0.5$$
$$b_p = 0.5\ Z/A'$$
$$b_\alpha = 0.5\ (0.5\ f\ Z/A')$$

where A' = N + Z + 0.5 fZ and the fraction 0.5 accounts for the incident neutron.

The value of k has been determined by Kalbach[6] to be 400 MeV^3. This value depends strongly on the level density parameters. Since the level densities we used here have strong pairing corrections, the value of k is expected to increase. The value k = 700 MeV^3 was determined by fitting the high-energy half of the 14.6-MeV ^{56}Fe(n,xp) spectrum measured by Grimes *et al.*[11] as shown in Fig. 1. The (n,xn) spectrum, measured by Hermsdorf *et al.*[12] and integrated over angle by Hetrick *et al.*[17] was not used for determining the value of k because of possible presence of collective excitations. We have reported[18] DWBA calculations for 15 of the 26 discrete levels up to 4.5 MeV in 14.5-MeV ^{56}Fe(n,n') reactions. The dashed histograms in the calculated (n,xn) spectrum in Fig. 1 represent such DWBA calculations. Collective strengths in higher-energy levels may not be negligible, making the determination of the parameter k on (n,xn) spectrum somewhat uncertain.

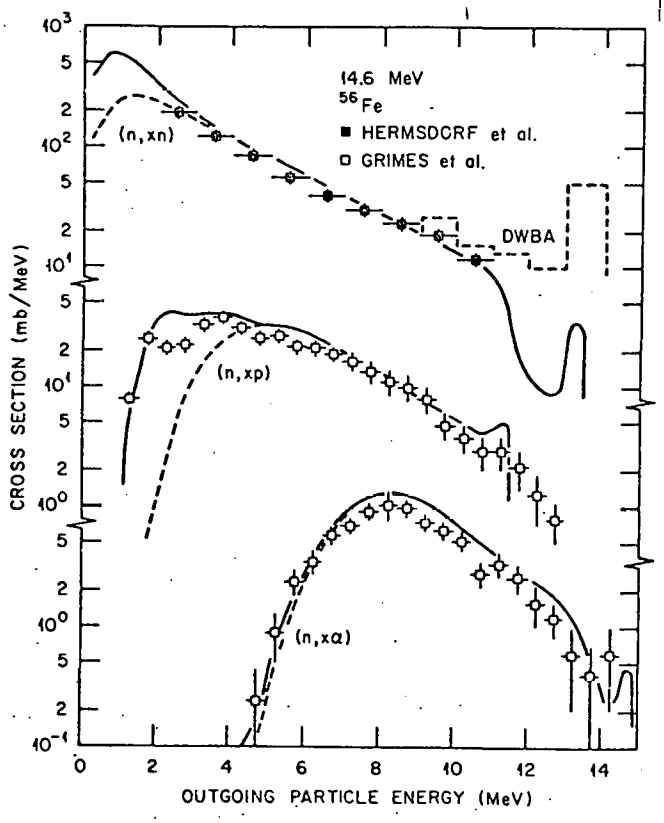

Fig. 1. Calculated and experimental n, p, α production spectra from 14.6-MeV neutrons on ^{56}Fe. The solid curves are calculations. The dashed curves include calculated contributions from the binary step only. The histograms represent DWBA calculations of (n,n') cross sections for 15 discrete levels.

The (n,xn) spectra measured by Hermsdorf *et al.* are the only set covering all thirteen isotopes studied here. Five other sets of measurements for ^{56}Fe, considered previously,[18] are omitted for clarity. The (n,xp) and (n,xα) spectra measured by Grimes *et al.* are probably the only high quality data available.

After the value of k was determined, the value f = 0.2 was found from the high-energy tail of the ^{56}Fe(n,xα) spectrum shown in Fig. 1. This value of f increases the tail of the (n,xα) spectrum near 13 MeV by only 25% from a case calculated with f = 0, thus is weakly determined. A survey[19] of previous calculations for heavier isotopes (A > 100), for which the precompound effect is more pronounced, shows large fluctuations of f with A and shell structures.

With the above parameters, we proceed to predict similar spectra for the other twelve isotopes: ^{27}Al, ^{46,48}Ti, ^{51}V, ^{50,52}Cr, ^{54}Fe, ^{58,60}Ni, ^{63,65}Cu, and ^{93}Nb. Some of the results (^{27}Al, ^{54}Fe, ^{63}Cu, ^{93}Nb) are compared in Fig. 2 with experimental data. The (n,xn) data are for natural elements, so are shown separately in Fig. 3.

The calculated (n,xn) spectra represent sums of partial spectra from (n,n'), 2x(n,2n), (n,pn), and (n,αn) reactions. The (n,xp) spectra are sums of (n,p), (n,pn), and (n,np). The (n,xα) spectra are sums of (n,α), (n,αn), and (n,nα). The dashed curves in Fig. 2 include calculated results from the first step only. The high-energy edge in each (n,xn) spectrum represents the position of the first excited state

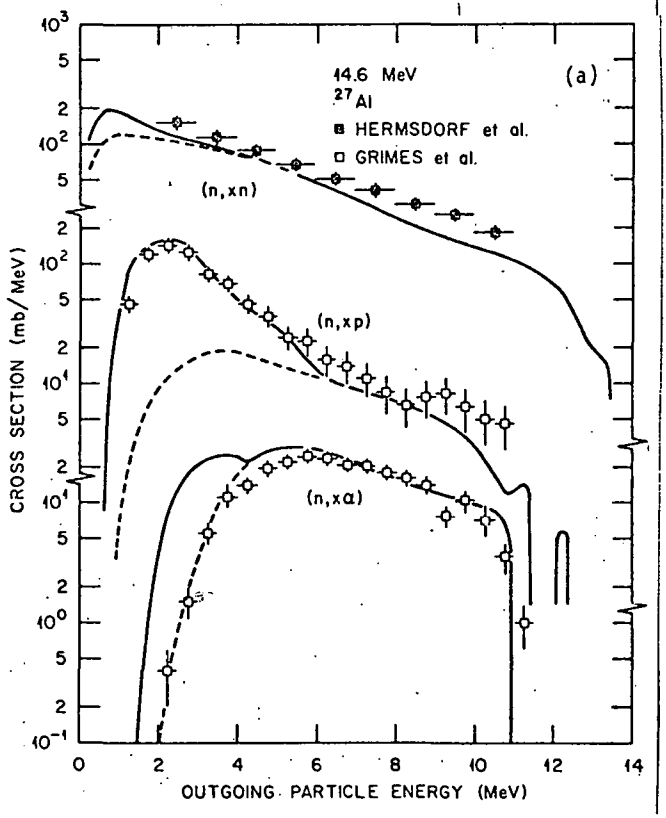

Fig. 2. Calculated and experimental n, p, α production spectra from 14.6-MeV Neutrons on (a) ^{27}Al, (b) ^{54}Fe, (c) ^{63}Cu, and (d) ^{93}Nb. The dashed curved include contributions from the binary step only.

in the residual nucleus in (n,n') reaction, while those in the (n,xp) and (n,xα) spectra correspond to the ground states. The dip in the high-energy tail, when

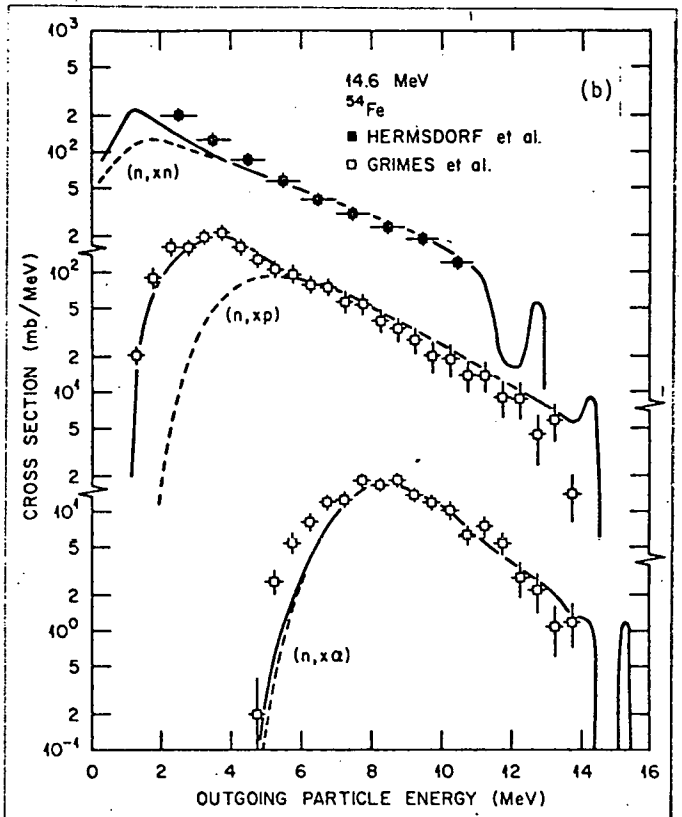

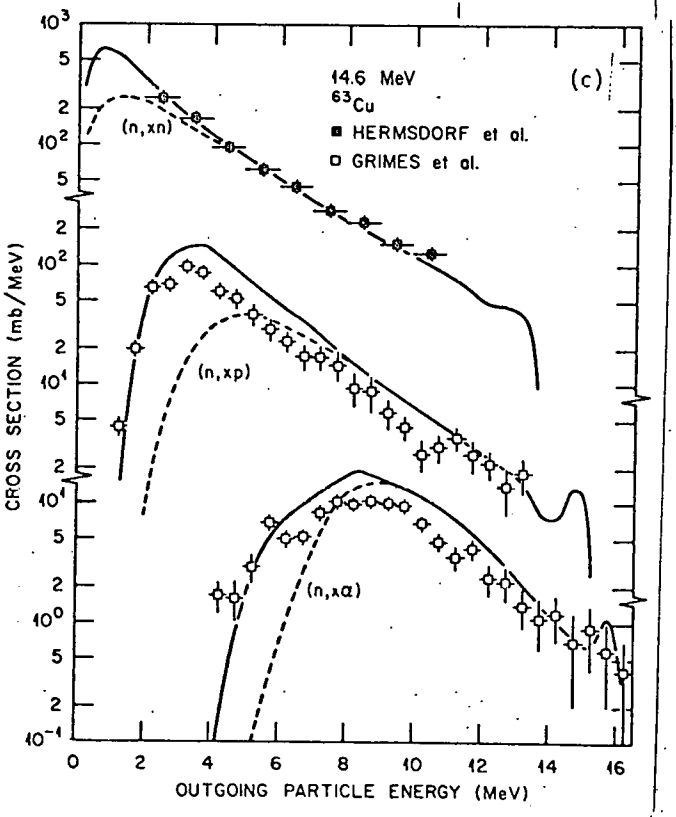

present, is from the odd-even shift, which is the most pronounced in even-even residual nucleus.

Best agreement between calculations and experiments is seen for the (n,xp) spectra. This is probably not surprising since the reactions comprising the (n,xp) spectra are rather pure compound and precompound combinations. The measured (n,xn) spectra contain

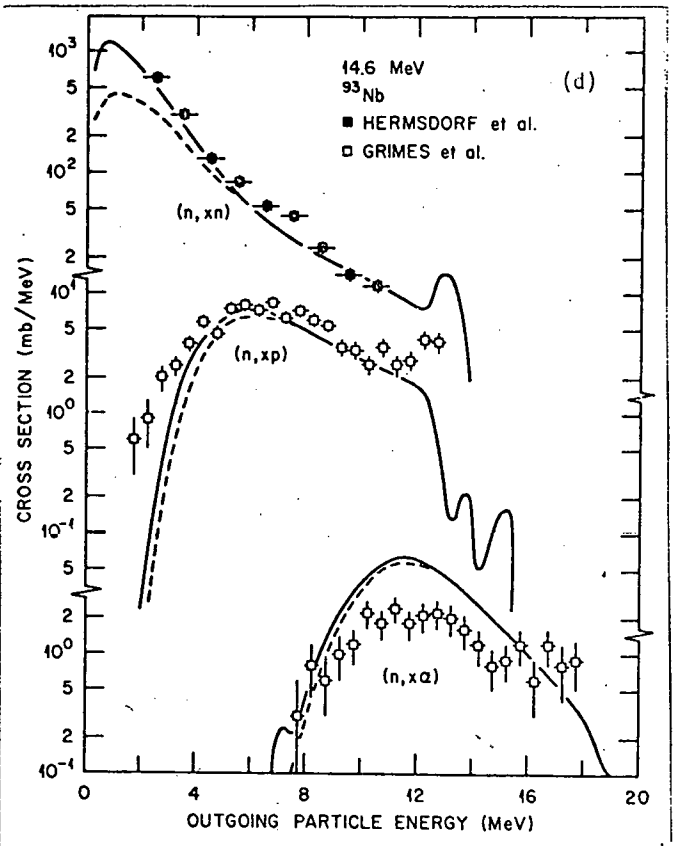

collective excitations. Although DWBA calculations are routinely performed for the low-lying discrete levels for cross-section evaluation works,[16,18,20] it is not straightforward to deal with collective excitations for the continuum states. However, in view of the reasonable agreement between calculated and measured (n,xn) spectra, the collective excitation in continuum states cannot be large in most cases. In several cases, the agreement between calculated and measured (n,xα) spectra is not quite satisfactory. Since the precompound effect is rather small in (n,α)reactions induced by 14.6-MeV neutrons, we speculate that the optical-model parameters used for alpha-particles are not valid for all the isotopes and energies, particularly for low-energy transitions. The conclusion by McFadden and Satchler[21] that a global set of optical-model parameters for alpha-particles could not be found has not yet been challenged.

Conclusion

Our consistent treatment of the compound and precompound reactions leads to a single model that reduces to the usual Hauser-Feshbach model at low energies where the precompound effects are negligible. A single set of parameters, including those for level densities, is used for both modes of reactions. For 14.6-MeV neutron-induced reactions, the second outgoing particle often sees only a few discrete levels in the residual nuclei. Therefore, the multi-step Hauser-Feshbach method is used for describing the tertiary reactions. For the same reason, spin populations in the intermediate nuclei are important, and are calculated with conservation of angular momentum in both modes of reaction.

Acknowledgements

The author wishes to thank D. M. Hetrick of Computer Science Division for making most of the calculations and plots, and Prof. C. Kalbach of Duke Univ. for providing the computer code PRECOA, and Dr.

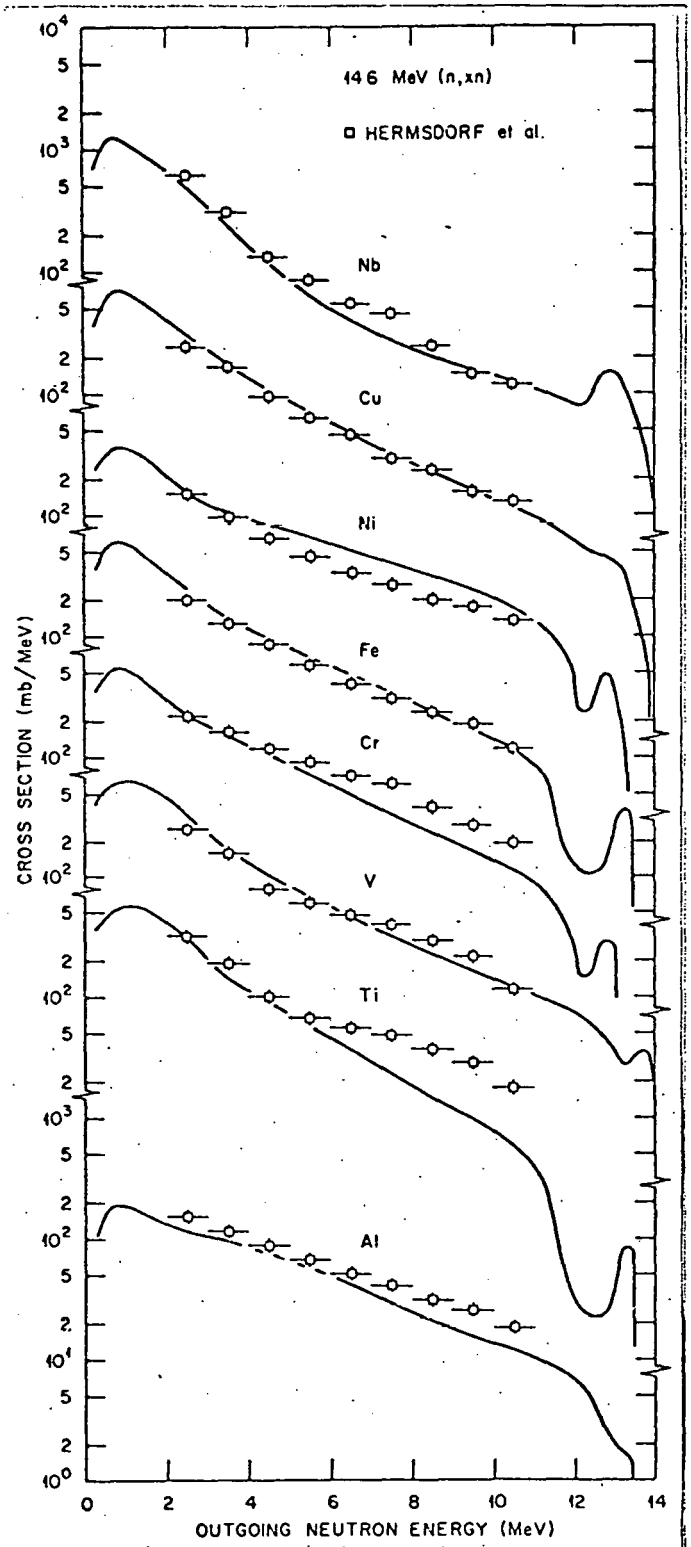

Fig. 3. Calculated and experimental neutron production spectra from 14.6-MeV neutrons on eight natural elements. See Figs. 1 and 2 for some of the results calculated for individual isotopes.

R. C. Haight of Lawrence Livermore Laboratory for sending experimental data prior to publication.

Research sponsored by the U.S. Department of Energy, Office of Basic Energy Sciences, under contract No. W-7405-eng-26 with Union Carbide Corporation.

References

1. M. R. Bhat and S. Pearlstein, Editors, "Symposium on Neutron Cross Sections from 10 to 40 MeV," held at Brookhaven National Laboratory, Upton, New York 11973, May 3-5, 1977, BNL-NCS-50681 (1977).
2. L. Stewart and E. D. Arthur, "Neutron Cross-Section Evaluation at High Energies - Problems and Prospects," p. 435, *ibid.*
3. C. Y. Fu, "Multi-Step Hauser-Feshbach Codes with Precompound Effects: A Brief Review of Current and Required Developments and Applications up to 40 MeV," p. 453, *ibid.*
4. W. Hauser and H. Feshbach, Phys. Rev. 87, 366 (1952).
5. C. Y. Fu, submitted to Phys. Rev.
6. I. Ribansky, P. Oblozinsky, and E. Betak, Nucl. Phys. A205, 545 (1973).
7. C. Kalbach, Z. Physik A283, 401 (1977).
8. F. C. Williams, Jr., Nucl. Phys. A166, 231 (1971).
9. A. Gilbert and A. G. W. Cameron, Can. J. Phys. 43, 1446 (1965).
10. A. Bohr and B. R. Mottelson, Nuclear Structure (W. A. Benjamin, Inc., New York, 1969), p. 169.
11. S. M. Grimes, R. C. Haight, K. R. Alvar, H. H. Barschall, and R. R. Borchers, Phys. Rev. C19, 2127 (1979). R. C. Haight and S. M. Grimes, Lawrence Livermore Laboratory Report UCRL-80235 (1977) and private communication.
12. D. Hermdsdorf, A. Meister, S. Sassonoff, D. Seeliger, K. Seidel, and F. Shahin, Zentralinstitut für Kernforschung, Rossendorf Bei Dresden, ZfK-277 (Ü), (1975).
13. D. Wilmore and P. Hodgson, Nucl. Phys. 55, 673 (1964).
14. F. D. Becchetti and G. W. Greenlees, Phys. Rev. 182, 1190 (1969).
15. J. R. Huizenga and C. J. Igo, Nucl. Phys. 29, 462, (1962).
16. C. Y. Fu, Atomic Data and Nucl. Data Tables 17, 127 (1976).
17. D. M. Hetrick, D. C. Larson, and C. Y. Fu, Oak Ridge National Laboratory Report ORNL/TM-6637, ENDF-280 (1979).
18. C. Y. Fu, in *Nuclear Cross Sections and Technology*, Proceedings of a Conference, Vol. I, p. 325, National Bureau of Standards Special Publication SP-425, Washington, D. C., 1975.
19. H. J. Mang, in *Proceedings of the Second International Conference on Clustering Phenomena in Nuclei*, Vol. II, p. 601, College Park, Maryland, 1975.
20. C. Y. Fu and F. G. Perey, Atomic Data and Nucl. Data Tables 16, 409 (1975).
21. L. McFadden and G. R. Satchler, Nucl. Phys. 84, 177 (1966).